jth

ORIGINAL ARTICLE

COVID-19 patient fibrinogen produces dense clots with altered polymerization kinetics, partially explained by increased sialic acid

Nina Moiseiwitsch[1,2] | Nicole Zwennes[2,3] | Fania Szlam[4] | Roman Sniecinski[4] | Ashley Brown[1,2,5]

[1]Joint Department of Biomedical Engineering of University of North Carolina – Chapel Hill and North Carolina State University, Raleigh, North Carolina, USA

[2]Comparative Medicine Institute, North Carolina State University, Raleigh, North Carolina, USA

[3]Department of Biological Sciences, North Carolina State University, Raleigh, North Carolina, USA

[4]Department of Anesthesiology, Emory University School of Medicine, Atlanta, Georgia, USA

[5]Department of Material Science and Engineering, North Carolina State University, Raleigh, North Carolina, USA

Correspondence
Ashley Brown, Joint Department of Biomedical Engineering, North Carolina State University and University of North Carolina at Chapel-Hill, 1001 William Moore Dr, Raleigh, NC 27606, USA.
Email: aecarso2@ncsu.edu

Funding information
NIH, Grant/Award Number: 1F30HL163869, 5T34GM131947, R01HL146701 and UL1-TR002378

Abstract

Background: Thrombogenicity is a known complication of COVID-19, resulting from SARS-CoV-2 infection, with significant effects on morbidity and mortality.

Objective: We aimed to better understand the effects of COVID-19 on fibrinogen and the resulting effects on clot structure, formation, and degradation.

Methods: Fibrinogen isolated from COVID-19 patients and uninfected subjects was used to form uniformly concentrated clots (2 mg/ml), which were characterized using confocal microscopy, scanning electron microscopy, atomic force microscopy, and endogenous and exogenous fibrinolysis assays. Neuraminidase digestion and subsequent NANA assay were used to quantify sialic acid residue presence; clots made from the desialylated fibrinogen were then assayed similarly to the original fibrinogen clots.

Results: Clots made from purified fibrinogen from COVID-19 patients were shown to be significantly stiffer and denser than clots made using fibrinogen from noninfected subjects. Endogenous and exogenous fibrinolysis assays demonstrated that clot polymerization and degradation dynamics were different for purified fibrinogen from COVID-19 patients compared with fibrinogen from noninfected subjects. Quantification of sialic acid residues via the NANA assay demonstrated that SARS-CoV-2-positive fibrinogen samples contained significantly more sialic acid. Desialylation via neuraminidase digestion resolved differences in clot density. Desialylation did not normalize differences in polymerization, but did affect rate of exogenous fibrinolysis.

Discussion: These differences noted in purified SARS-CoV-2-positive clots demonstrate that structural differences in fibrinogen, and not just differences in gross fibrinogen concentration, contribute to clinical differences in thrombotic features associated with COVID-19. These structural differences are at least in part mediated by differential sialylation.

KEYWORDS
coagulopathy, COVID-19, fibrinogen, sialic acid, thrombosis

----

1 | INTRODUCTION

As of February 2022, an estimated 58% of Americans have had active SARS-CoV-2 infection, resulting in COVID-19 illness.[1] Although the initial scientific perception of COVID-19 was that of a severe short-term respiratory disease, recent studies have uncovered the short- and long-term effects of COVID-19 on the vasculature and blood. A European network cohort study estimated that up to 1% of COVID-19 cases result in severe thromboembolic events within the first 90 days following injury, and numerous studies have found that thromboembolic events are more common in the context of COVID-19 and are associated with increased mortality and the need for intensive care unit (ICU)-level patient care.[2–8] Current data suggest that the pro-thrombotic aspects of COVID-19 symptoms are multifactorial in origin, with endothelial and platelet dysfunction, significant inflammation, and blood stasis all playing a role.[8–13] This results in both vessel damage and increased risk of thrombotic complications. Clotting has also been implicated in the pathogenesis of post-acute sequelae of COVID-19, colloquially referred to as "long COVID." It is hypothesized that the formation of fibrin amyloid clots that are resistant to fibrinolysis among long COVID sufferers leads to reduced blood flow in small vessels, and thus reduced gas exchange, leading to the common symptoms of fatigue, "brain fog," and shortness of breath.[14,15]

In a case–control study of clot formation from platelet poor plasma, patients being treated for COVID-19 in an ICU were found to produce clots with demonstrably increased fibrin network density and decreased susceptibility to fibrinolysis.[16,17] SARS-CoV-2–infected patients have also been shown to have increased plasma concentrations of fibrinogen and factor V.[17,18] Thus, with the data collected from studies published thus far, differences in platelet poor plasma clotting characteristics cannot be determined to be the result of functional or structural differences in clotting factors or simply the result of increased concentrations of these factors.

Fibrinogen (factor I) is a soluble glycoprotein complex found in the blood that is essential to clot formation. Upon cleavage by the serine protease thrombin, soluble fibrinogen is turned into insoluble fibrin. Fibrin polymerizes to form a mesh-like network that provides the structural foundation for a clot. Produced by the liver, fibrinogen is subject to posttranslational modification in a number of different pro-thrombotic disease states, including disseminated intravascular coagulation, liver disease, and uncontrolled diabetes mellitus.[19] One such form of posttranslational modification is sialylation, wherein sialic acid residues are added to the ends of carbohydrate chains of fibrinogen. As sialic acid residues alter calcium binding to fibrinogen, they influence the polymerization and structure of fibrin clots.[20,21] Differential sialylation is known to play a role in the pro-thrombotic associations of liver disease, and furthermore, to account for some of the structural and functional differences between adult and neonatal fibrinogen.[22,23]

Given the known effects of COVID-19 on the functionality of other blood components, and the known posttranslational modifications of fibrinogen in the context of other pro-thrombotic disease states, we were interested in comparing the structure and function of fibrinogen isolated from COVID-19 patients with the fibrinogen properties of noninfected subjects. In this study, we also examined the role of sialic acid residues on the fibrin clot properties in COVID-19 plasma. We hypothesized that COVID-19 fibrin clots would display differences in structure and function, and that removal of sialic acid residues would lead to resolution of structural and kinetic differences observed in COVID-19 fibrin clots. We explored this hypothesis through analysis of structural and polymerization/degradation properties of normal and desialylated COVID-19 fibrinogen and compared them with normal and desialylated noninfected adult controls.

Essentials

- Thrombotic complications are common during and following SARS-Cov-2 infection resulting in COVID-19 illness, with significant effects on morbidity and mortality.
- Fibrinogen was isolated from plasma collected from patients being treated for COVID-19 at Emory University Hospital.
- Clots made from fibrinogen collected from COVID-19 patients were denser, stiffer, less porous, and displayed altered polymerization and degradation profiles.
- Fibrinogen from COVID-19 patients is structurally different, leading to increased thrombogenicity.

2 | MATERIALS AND METHODS

2.1 | Isolation of fibrinogen

This study was approved by the Emory University institutional review board and written consent was obtained from all subjects or their proxies. Samples of whole blood were collected from adult patients with SARS-CoV-2 viral infection confirmed by polymerase chain reaction testing who were admitted to the ICU at Emory University Hospital with a primary diagnosis of respiratory failure. Patients on coumadin before hospital admission were excluded. Control samples were obtained from SARS-CoV-2–negative patients admitted to the ICU following surgery (ICU control) or healthy volunteers (healthy control), who were screened for any preexisting hematological abnormalities. From here, when referring to the combination of these two subgroups, we will use the term "control subjects." Samples were collected for this pilot study based on availability, with samples collected from nine COVID+ patients (Table 1) and six uninfected subjects (three ICU control and three healthy control). All patient samples were deidentified before analysis and researchers were blinded to group during data analysis. Following collection in either citrated or EDTA tubes, samples were immediately centrifuged at 2000g for 20 min. The resultant platelet poor plasma was stored at −80°C until use. For some samples, blood was collected in duplicate

TABLE 1 Demographic data from sampled COVID-19 patients, control ICU patients, and healthy control patients

	COVID-19 samples (n = 9)	Control ICU samples (n = 3)	Healthy control samples (n = 3)
Female	1 (11.1%)	1 (33.3%)	1 (33%)
Median age (range)	65 (56–76)	65 (39–67)	34 (31–44)
Median ICU day (range)	2 (1–7)	1 (1–20)	Not applicable
Intubated (percentage)	7 (77.8%)	3 (100%)	Not applicable
Median D-dimer (range) in ng/ml Fibrinogen equivalent units	1304 (693–60000)	Not available	Not available
Median fibrinogen (range), mg/dl	769 (391–860)	Not available	Not available
Median Sequential Organ Failure Assessment Score (range)	5 (2–9)	4 (2–5)	Not applicable
Samples collected EDTA	9 (100%)	0 (0%)	3 (100%)

EDTA and citrate tubes, from which we performed head-to-head comparisons of a subset of our assays to ensure that initial collection in citrate versus EDTA did not affect our results from the isolated fibrinogen. Fibrinogen was isolated from patient samples of platelet poor plasma using ethanol precipitation, after which all fibrinogen samples were resuspended in sodium citrate solution (20 mM).[24–26] Previous work from our laboratory has shown that this method results in the overwhelming precipitation of fibrinogen, although trace amounts of factor XIII, fibronectin, and von Willebrand factor are also present alongside the extracted fibrinogen.[23]

2.2 | Quantification of fibrinogen sialic acid residues

Cleavage of sialic acid residues from fibrinogen was achieved via neuraminidase digestion for samples collected from both COVID-19 patients and control subjects.[27] Fibrinogen solutions were kept in single-source solutions, with no within-group sample pooling. Fibrinogen solutions (5 mg/ml) were incubated with neuraminidase (0.025 U/ml; MilliporeSigma, Darmstadt, Germany) for 4 h at 25°C, at which point samples were filtered with 100-kDa molecular weight cutoff Pall Nanosep devices and stored at −80°C. Sialic acid (NANA) assay kit (Abcam) was used to quantify fibrinogen sialic acid content. This assay is able to detect and quantify unbound sialic acid residues through their oxidation and subsequent stoichiometric interaction with a chemical probe to yield an output that has an absorbance maximum at 570 nm. Digestion was confirmed through assay of sialic acid concentration before and after incubation with neuraminidase.

2.3 | Characterization of fibrin matrix structure via confocal and cryogenic scanning electron microscopy

Fibrin clot structure was imaged and characterized using confocal microscopy and cryogenic scanning electron microscopy (cryoSEM).[23,28–32] For confocal microscopy, 50 μl clots consisting of 2 mg/ml purified fibrinogen (Fisher Scientific), 1 M N-2-hydroxyethylpiperazine-N′-2-ethanesulfonic acid (HEPES) buffer (5 mM calcium, 7.4 pH), 10 μg/ml Alexa 488–labeled adult fibrinogen

(for visualization; Thermo Fisher Scientific), and 0.5 U/ml thrombin (Fisher Scientific, Waltham, MA, USA), were produced between a glass slide and coverslip. After allowing 2 hours for polymerization, clots were imaged using a Zeiss Laser Scanning Microscope (LSM 710, Zeiss Inc.) at 40× magnification. Two clots were formed per subject sample, and a minimum of three random 5.67 μm z-stacks were acquired for each clot. ImageJ (National Institutes of Health) was used to produce z-stack projections, which were then analyzed using MATLAB to quantify fiber density. For cryoSEM imaging, 150-μl clots consisting of 2 mg/ml purified fibrinogen in 1 M HEPES buffer, and polymerized with 0.5 U/ml thrombin were formed in a 0.6 ml Eppendorf tube and allowed to polymerize for 12 h. Clots were rapidly plunge-frozen in super-cooled liquid nitrogen, etched for 10 min, and sputter-coated with gold. Imaging was performed at 1000×, 1500×, 2000×, and 2500× on two clots per group (COVID-19 vs. control, ± sialic acid), in three random locations within the clot using a JEOL scanning electron microscope (JEOL JSM-7600F, JEOL USA). ImageJ was used to perform image segmentation and then analyze pore size, percent porosity, fiber length, fiber intersections, and fiber diameter. CryoSEM was chosen because the snap frozen sample preparation central to cryoSEM allows for greater preservation of natural clot structure because traditional SEM requires sample drying, which can greatly affect the porosity, pore size, and overall appearance of low-density hydrogels, such as natural fibrinogen clots.

2.4 | Analysis of mechanical clot properties via atomic force microscopy

Clot stiffness was quantified using atomic force microscopy. Briefly, 50-μl clots were formed using 2 mg/ml purified fibrinogen, 1 M HEPES buffer, and 0.5 U/ml thrombin, and allowed to polymerize on a charged glass slide for 2 h. Atomic force microscopy (Asylum MFP3D-Bio; Asylum Research) imaging proceeded in force contact mode with partial chromium/gold coating of the cantilever on the detector side and a particle diameter of 1.98 μm (NanoAndMore). Cantilevers used had a force constant of 0.01 N/m to allow for high sensitivity when measuring soft biological materials. Three 20×20 μm force maps were obtained per clot, with preference for

the center of each clot to avoid the variation introduced by edge effects. Each force map consisted of a 16×16 array of contact points, which were fitted to a Hertz model to determine the elastic modulus for each point, and the average elastic modulus from these 256 contact points was recorded.

2.5 | Analysis of thrombin-initiated fibrinogen polymerization kinetics

A thrombin-initiated fibrin polymerization assay was used to determine clotting times and clot turbidity for purified fibrinogen from COVID-19 patients and control subjects, and neuraminidase-digested purified fibrinogen from COVID-19 patients and control subjects. Fibrin clots (80 μl) were produced in a 96-well plate with purified fibrinogen (COVID-19 vs control, ± neuraminidase; 2 mg/ml), 1 M HEPES buffer, with polymerization initiated through the addition of thrombin (0.5 U/ml). A plate reader (Infinite 200 Pro; TECAN) was used to create turbidity curves by reading the absorbance at 350 nm every 45 s for 3 h. Turbidity curves were used to determine polymerization time (time to reach half of the maximum turbidity value), and polymerization rate (slope at half of the maximum turbidity value). Humidity measurements and volume loss analyses were performed to ensure that sample drying was not a concern during any of the assays performed over multiple hours. Samples were run in duplicate and data were excluded if bubble formation caused improper absorbance readings. Turbidity curves were truncated after 6000 s (100 min), as full polymerization had already been achieved within the first hour of the assay's duration.

2.6 | Analysis of endogenous fibrin degradation dynamics

An endogenous fibrinolysis assay[29] was used to evaluate clot formation and degradation in the concurrent presence of thrombin, plasmin (Invitrogen), and tissue plasminogen activator (tPA; Sigma-Aldrich) for purified fibrinogen from COVID-19 patients and control subjects, and neuraminidase-digested purified fibrinogen from COVID-19 patients and control subjects. Fibrin clots (100 μl) were formed in a 96-well plate with purified fibrinogen (2 mg/ml), 1 M HEPES buffer, and the addition of thrombin (0.5 U/ml), plasminogen (10.8 μg/ml), and tPA (0.29 mg/ml). Turbidity curves were generated by using a plate reader to measure absorbance at 350 nm every 45 s for 2.5 h. Analysis of turbidity curves included area under the curve, maximum absorbance, rate of polymerization (determined by the rate of change in turbidity at one-half the maximum absorbance value), and instantaneous rate of degradation (determined by the rate of change in turbidity at the second occurrence of one-half the maximum absorbance value). Data collection occurred in duplicate for each sample, and data were excluded if bubbles formed during polymerization, leading to erroneous absorbance readings. Turbidity

curves were truncated after 6000 s (100 min) because steady state was achieved within an hour of the assay's start time.

2.7 | Analysis of exogenous fibrin degradation kinetics

An exogenous fibrinolysis assay was used to determine clot degradation kinetics through the external application of a natural fibrinolytic agent to fully polymerized clots formed from purified fibrinogen from COVID-19 patients and control subjects, and neuraminidase-digested purified fibrinogen from COVID-19 patients and control subjects. Fibrin clots (80 μl) were formed in a 96-well plate as in the previously described thrombin-initiated fibrin polymerization assay and allowed to polymerize for 3 h. At this point, degradation was initiated through the overlay of an 80-μl plasmin (0.5 U/ml; Invitrogen) solution. A plate reader was used to create degradation curves by reading the absorbance at 350 nm every 45 s for 8 h. Turbidity curves were used to determine degradation time (time to reach half of the initial turbidity value), and instantaneous degradation rate (slope at half of the initial turbidity value). Samples were run in duplicate and if bubble formation caused erroneous absorbance readings, data were excluded. Turbidity curves were truncated to highlight the first 1 h and 45 min of degradation to preserve as much visible detail because steady state was achieved by the end of this period.

2.8 | Statistical analysis

GraphPad Prism (GraphPad) was used to perform statistical analysis, and biostatisticians were consulted where appropriate. Before parametric testing, all groups were tested for normality using the Shapiro–Wilk test. Data were analyzed via unpaired, two-tailed Student t test with Welch's correction, comparing measurements for purified fibrinogen from COVID-19 patients versus control subjects, and for comparing measurements for neuraminidase-digested purified fibrinogen from COVID-19 patients versus control subjects. Instantaneous degradation rates from the exogenous fibrinolysis assay were analyzed using Brown-Forsythe and Welch's ANOVA tests. Where appropriate, ROUT analysis ($Q = 0.5\%$) was used to identify outliers for exclusion. Statistical significance was defined as $p < .05$, and data are reported as average ± SD.

3 | RESULTS

Samples were collected from a total of 9 COVID-19 patients being treated for active SARS-CoV-2 infection in the ICU of Emory University Hospital. Of these patients, none suffered documented thrombotic or thromboembolic complications, although two ultimately died in the hospital from complications from COVID-19. Six control samples were also collected, consisting of an even split between healthy controls and postsurgical ICU patients that tested

negative for SARS-CoV-2 infection. Composite sample demographic data are detailed in Table 1.

3.1 | Characterization of fibrin clot mechanical properties

Atomic force microscopy was used to characterize the mechanical properties of clots made from purified fibrinogen from COVID-19 patients and control subjects. These data demonstrated that COVID-19 clots were significantly stiffer than control clots (control, 1231 ± 206 Pa; COVID-19, 1884 ± 688 Pa; $p = .0034$; Figure 1).

3.2 | Characterization of fibrin matrix structure

Fiber density, as measured by confocal images, was found to be significantly greater for clots made from COVID-19 fibrinogen (control, 0.41 ± 0.11 black pixels/white pixels; COVID-19, 1.17 ± 0.33 black pixels/white pixels; $p = .0016$) (Figure S1). COVID-19 clots were found to be generally denser, but were also found to contain pockets of highly dense fibrinogen. At least two representative samples from each group were chosen for cryoSEM imaging to allow for more intuitive visualization of the clot structure and porosity analysis (Figure 2). In the clots made from COVID-19 fibrinogen, pore size was found to be significantly smaller (control, 17.8 ± 32.6 μm^2; COVID-19, 7.75 ± 14.1 μm^2; $p < .0001$) and percent porosity was significantly lower (control, $66.2 \pm 3.79\%$ porosity; COVID-19, $41.8 \pm 9.99\%$ porosity;

$p = .0034$). In COVID-19 fibrinogen clots, fiber length was found to be significantly smaller (control, 10.4 ± 7.97 μm; COVID-19, 5.44 ± 3.11 μm; $p < .0001$), whereas fiber width (control, 2.14 ± 0.884 μm; COVID-19, 5.16 ± 2.78 μm; $p < .0001$) and fiber intersections per 100 μm^2 (control, 22.4 ± 1.28 intersections; COVID-19, 39.32 ± 11.76 intersections; $p < .0012$) were both significantly higher (Figure 2). These results are consistent with the data collected using confocal imaging. These data also align with the increased density noted on atomic force microscopy. Desialylation appears to have increased the fiber density of control clots noted on confocal. This is could be due to differences in the location and structural function of the sialic acid residues between control and COVID-19 fibrinogen.

3.3 | Characterization of fibrinogen sialic acid content

Quantification of sialic acid (SA) residues using neuraminidase digestion and subsequent sialic acid (NANA) assay demonstrated that COVID-19 fibrinogen had significantly greater sialic acid residue concentration than Control fibrinogen (Control, 5.44 ± 2.28 nmol SA/well; COVID-19, 8.63 ± 2.02 nmol SA/well; $p = .022$) (Figure 2).

3.4 | Effects of sialic acid on fibrin matrix structure

Confocal microscopy and cryoSEM data demonstrated a resolution of differences in fiber density between COVID-19 and control
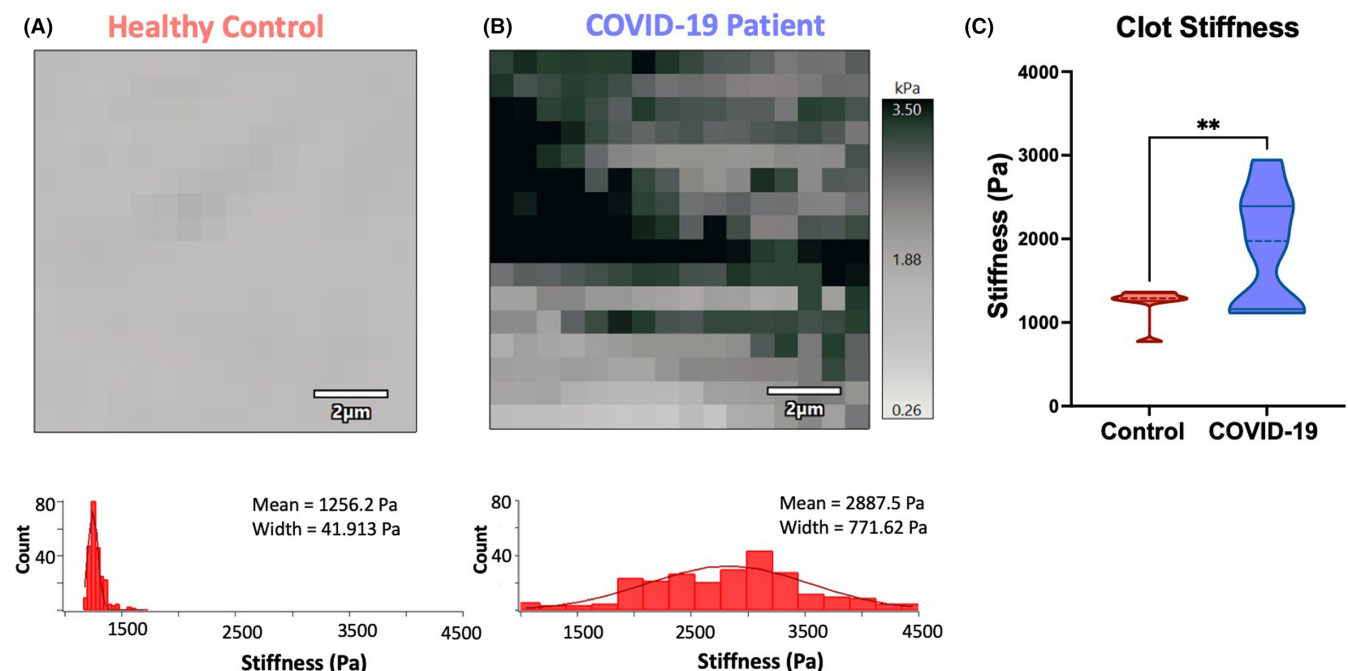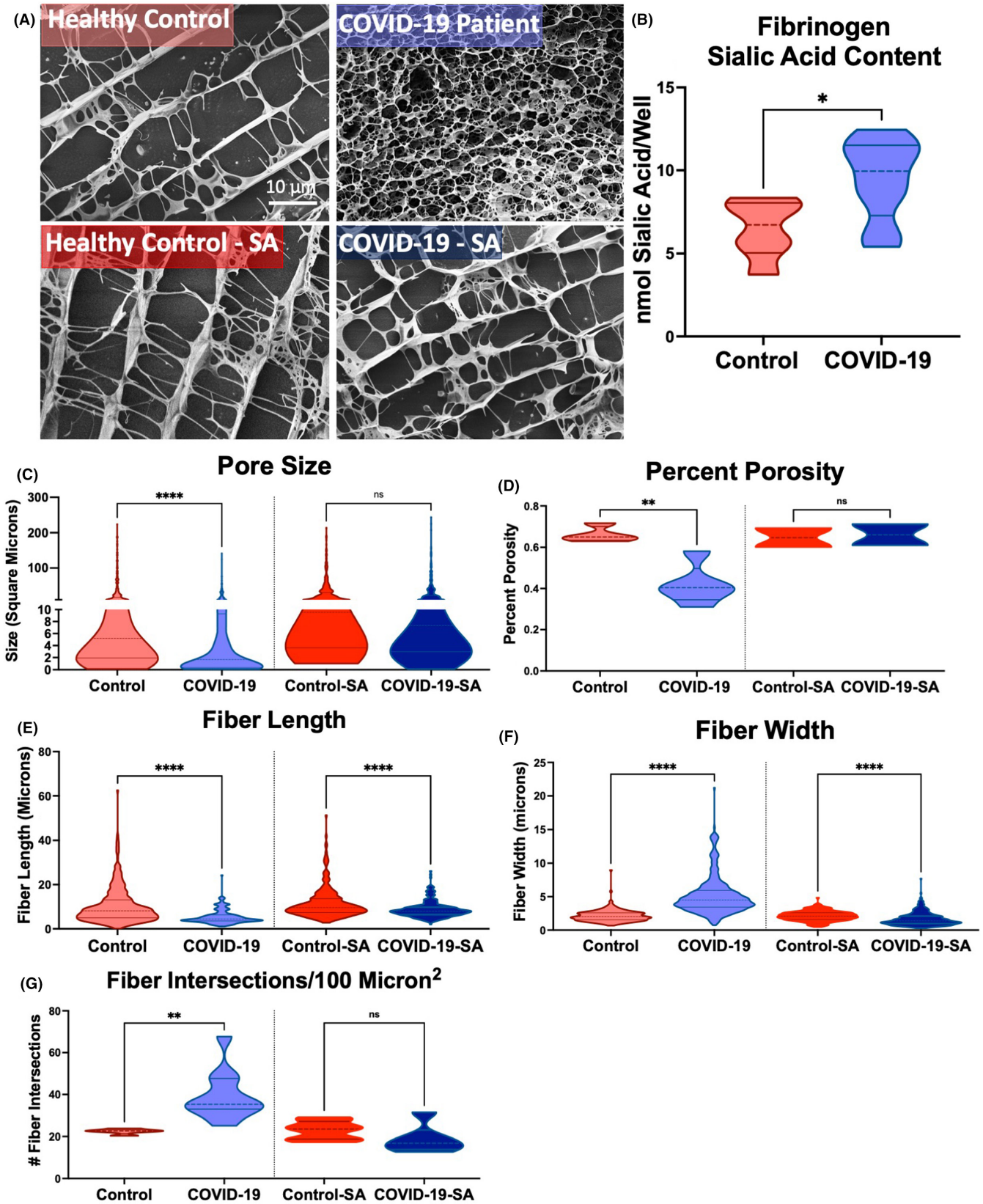

FIGURE 1 Representative fibrin clot force maps and mean clot stiffness. (A) Representative atomic force microscopy force map of a clot made with purified fibrinogen (2 mg/ml) from a healthy control subject. (B) Representative atomic force microscopy force map of a clot made with purified fibrinogen (2 mg/ml) from a COVID-19 patient. Scale bars = 2 μm. (C) Comparison of mean clot stiffness of COVID– purified fibrinogen clots versus COVID+ purified fibrinogen clots. **$p < .01$.

(A) Healthy Control, COVID-19 Patient, Healthy Control - SA, COVID-19 - SA

(B) Fibrinogen Sialic Acid Content

(C) Pore Size

(D) Percent Porosity

(E) Fiber Length

(F) Fiber Width

(G) Fiber Intersections/100 Micron^2

groups (control, 0.73 ± 0.26 black pixels/white pixels; COVID-19, 0.91 ± 0.17 nmol black pixels/white pixels; $p = .17$). After removal of SA residues via neuraminidase digestion, hyperdense fibrin pockets were no longer seen in confocal images of COVID-19 desialylated fibrin clots. The same representative subject samples

chosen for baseline cryoSEM imaging were chosen for imaging after desialylation. Resolution of density differences are clearly visible in these representative images (Figure 2). Following neuraminidase digestion, no differences were found in pore size (control, 23.2 ± 33.1 μm^2; COVID-19, 20.2 ± 31.2 μm^2; $p = .15$) or

FIGURE 2 Representative fibrin clot structure and sialic acid content. (A) Representative cryoSEM images of purified fibrinogen clots. Clockwise from top left: clot using purified fibrin from healthy control, clot using purified fibrin from COVID-19 patient, clot using desialylated purified fibrin from COVID-19 patient, clot using desialylated purified fibrin from healthy control. Both representative healthy control clots are made from fibrinogen from the same patient. Both representative COVID-19 clots are made from fibrinogen from the same patient. Contrast has been adjusted to allow for better visualization. Scale bar = 10 μm. (B) Comparison of mean sialic acid content of purified fibrinogen samples from control and COVID-19 subjects. (C) Comparison of mean pore size of fibrinogen clots from control and COVID-19 samples. (D) Comparison of mean percent porosity of fibrinogen clots from control and COVID-19 samples. (E) Comparison of fibrinogen fiber lengths of fibrinogen clots from control and COVID-19 samples. (F) Comparison of fibrinogen fiber widths of fibrinogen clots from control and COVID-19 samples. (G) Comparison of mean fiber intersections per $100\,\mu m^2$ of fibrinogen clots from control and COVID-19 samples. $*p<.05$, $**p<.01$, $****p<.0001$.

percent porosity (control, 64.7 ± 6.44 percent porosity; COVID-19, 66.10 ± 7.27 percent porosity; $p = .86$) between COVID-19 and control fibrinogen (Figure 2). Comparison of quantification from images of COVID-19 and desialylated COVID-19 fibrinogen clots demonstrated a significant increase in pore size following desialylation ($p<.0001$) and a significant increase in percent porosity ($p = .0445$). In confocal images, desialylation resulted in lowered fiber density from the COVID-19 group, although this did not reach significance ($p = .132$; Figure S1). Following neuraminidase digestion, COVID-19 fibrinogen clots were noted to have gone from having significantly wider fibers to significantly thinner fibers when compared with desialylated control fibrinogen clots (control, $2.12\pm0.736\,\mu m$; COVID-19, $1.66\pm0.995\,\mu m$; $p<.0001$) and went from having significantly more intersections per $100\,\mu m^2$ to having no significant difference in intersection count when compared to desialylated control fibrinogen clots (control, 23.0 ± 4.37 intersections; COVID-19, 18.72 ± 6.80 intersections; $p = .430$). Differences in fiber length remained (control, $11.5\pm6.88\,\mu m$; COVID-19, $8.74\pm3.68\,\mu m$; $p<.0001$), but the absolute difference between control and COVID-19 clots was lessened (Figure 2).

3.5 | Analysis of fibrinogen polymerization and clot degradation kinetics

Overall, COVID-19 samples demonstrated increased clot turbidity and clot polymerization rates, when compared with control samples. In an endogenous fibrinolysis assay, the turbidity curve for COVID-19 fibrin had significantly greater area under the curve (control, 201 ± 8.1 turbidity×s; COVID-19, 279 ± 16 turbidity×s; $p = .0010$), peak turbidity (control, 0.0481 ± 0.037 turbidity; COVID-19, 0.132 ± 0.073 turbidity; $p = .0089$), polymerization rate (control, 0.000181 ± 0.00017 Δturbidity/s; COVID-19, 0.000480 ± 0.00030 Δturbidity/s; $p = .0015$), and instantaneous degradation rate (control, -0.000144 ± 0.000083 Δturbidity/s; COVID-19, 0.000285 ± 0.00019 Δturbidity/s; $p = .0084$) (Figure 3). The COVID-19 clots formed faster, and clots remained present for longer despite their faster instantaneous degradation rates because of their increased maximum turbidity. An enzyme-initiated polymerization assay led to similar findings, with the turbidity curves for COVID-19 fibrin clots demonstrating significantly faster polymerization rates (control, 0.0000883 ± 0.000063 Δturbidity/s; COVID-19, 0.000159 ± 0.000078 Δturbidity/s; $p = .013$), and

significantly greater maximum turbidity values (control, 0.112 ± 0.092 turbidity; COVID-19, 0.283 ± 0.18 turbidity; $p = .0019$) (Figure 4). An exogenous fibrinolysis assay found no significant difference in instantaneous degradation rates between COVID-19 and control samples (control, -0.0000726 ± 0.000045 Δturbidity/s; COVID-19, -0.0000721 ± 0.000037 Δturbidity/s; $p = .98$) (Figure 5).

3.6 | Effects of sialic acid on fibrinogen polymerization and degradation kinetics

The influence of SA on fibrin polymerization was investigated through the repetition of the same assays used to probe polymerization and clot degradation kinetics with desialylated COVID-19 and control fibrinogen. Overall, it was found that although desialylation altered exogenous fibrinolysis kinetics, desialylation did not result in meaningful changes to enzyme-initiated polymerization kinetics or endogenous fibrinolysis. In the endogenous fibrinolysis assay, the turbidity curve for COVID-19 fibrin had significantly greater area under the curve (control, 133 ± 9.4 turbidity×s; COVID-19, 230 ± 16 turbidity×s; $p = .0002$), peak turbidity (control, 0.0828 ± 0.062 turbidity; COVID-19, 0.177 ± 0.090 turbidity; $p = .0054$), and faster polymerization rate (control, 0.000395 ± 0.00027 Δturbidity/s; COVID-19, 0.000662 ± 0.00030 Δturbidity/s; $p = .033$); however, instantaneous degradation rate was not significantly different (control, -0.000434 ± 0.00030 Δturbidity/s; COVID-19, -0.000634 ± 0.00021 Δturbidity/s; $p = .077$) (Figure 3). An enzyme-initiated polymerization assay led to similar findings, with the turbidity curves for COVID-19 fibrin clots demonstrating significantly greater maximum turbidity values (control, 0.137 ± 0.095 turbidity; COVID-19, 0.341 ± 0.17 turbidity; $p = .0003$) (Figure 4). Polymerization rates were also faster for COVID-19 samples, but this difference did not reach the level of significance (control, 0.000115 ± 0.000056 Δturbidity/s; COVID-19, 0.000160 ± 0.000082 Δturbidity/s; $p = .11$) (Figure 4). An exogenous fibrinolysis assay demonstrated that instantaneous degradation rates were significantly increased for desialylated COVID-19 samples, when compared with the behavior of the unaltered COVID-19 fibrinogen (COVID-19, -0.0000647 ± 0.000020 Δturbidity/s; desialylated COVID-19, -0.000126 ± 0.000073 Δturbidity/s; $p = .021$) (Figure 5). This suggests that the resolution in structural differences (density and porosity) as a result of desialylation was associated with increased rates exogenous fibrinolysis, but the
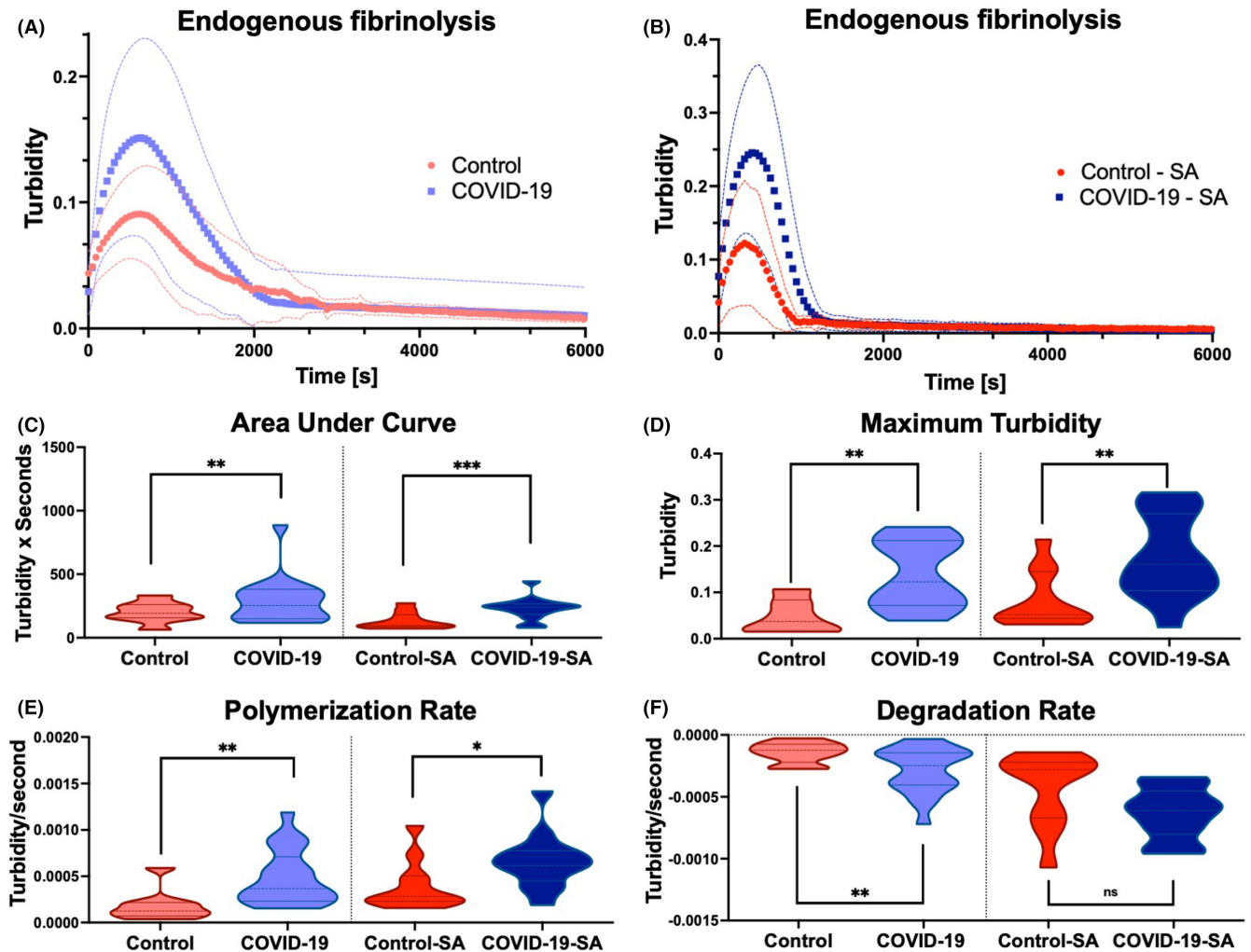
FIGURE 3 Endogenous fibrinolysis of COVID-19 and control fibrin clots, at baseline and after removal of sialic acid residues. (A) Endogenous fibrinolysis curves for COVID-19 and control fibrinogen. Thrombin (0.5 U/ml), plasminogen (10.8 μg/ml), and tPA (0.29 mg/ml), were added to 2 mg/ml fibrinogen, and a plate reader was used to produce turbidity curves demonstrating fibrin clot polymerization and endogenous degradation. $N = 6$–9 (B) Endogenous fibrinolysis curves for desialylated COVID-19 and control fibrinogen. $N = 6$–9. (C) Comparison of area under the curve for COVID-19 and control, and desialylated COVID-19 and control endogenous fibrinolysis turbidity curves. $N = 6$–9. (D) Comparison of maximum turbidity achieved for COVID-19 and control, and desialylated COVID-19 and control endogenous fibrinolysis turbidity curves. $N = 6$–9. (E) Comparison of polymerization rate for COVID-19 and control, and desialylated COVID-19 and control endogenous fibrinolysis turbidity curves. Polymerization rate was determined as the slope of the curve at half of the maximum turbidity. $N = 6$–9. (F) Comparison of instantaneous degradation rate achieved for COVID-19 and control, and desialylated COVID-19 and control endogenous fibrinolysis turbidity curves. Instantaneous degradation rate was determined as the slope of the curve at the second occurrence of half of the maximum turbidity. $N = 6$–9. *$p < .05$, **$p < .01$, ***$p < .005$.

differences in polymerization and degradation kinetics between COVID-19 and control fibrinogen is not fully explained by the differential sialylation of COVID-19 fibrinogen.

4 | DISCUSSION

Here, we characterized structural and kinetic differences between fibrinogen clots made from COVID-19 patient samples and samples from noninfected subjects. Our results indicate that COVID-19 fibrin clots are significantly stiffer, denser, and less porous than control fibrin clots. In terms of polymerization and degradation kinetics,

COVID-19 clots polymerize faster and reach a greater maximum turbidity. Further, the area under the curve, a good proxy for clot burden over time, was also significantly greater for COVID-19 clots. Through the use of consistent concentrations (2 mg/ml) of fibrinogen across all clots, we were able to isolate differences in clotting to structural differences in the glycoprotein complex, rather than in the concentration of fibrinogen, or other factors in the blood. Our findings therefore demonstrate that differences in clot structure and polymerization are not simply from the increased concentration of fibrinogen or other clotting factors in the plasma of COVID-19 patients, but rather from fundamental differences in the structure and functionality of their fibrinogen.
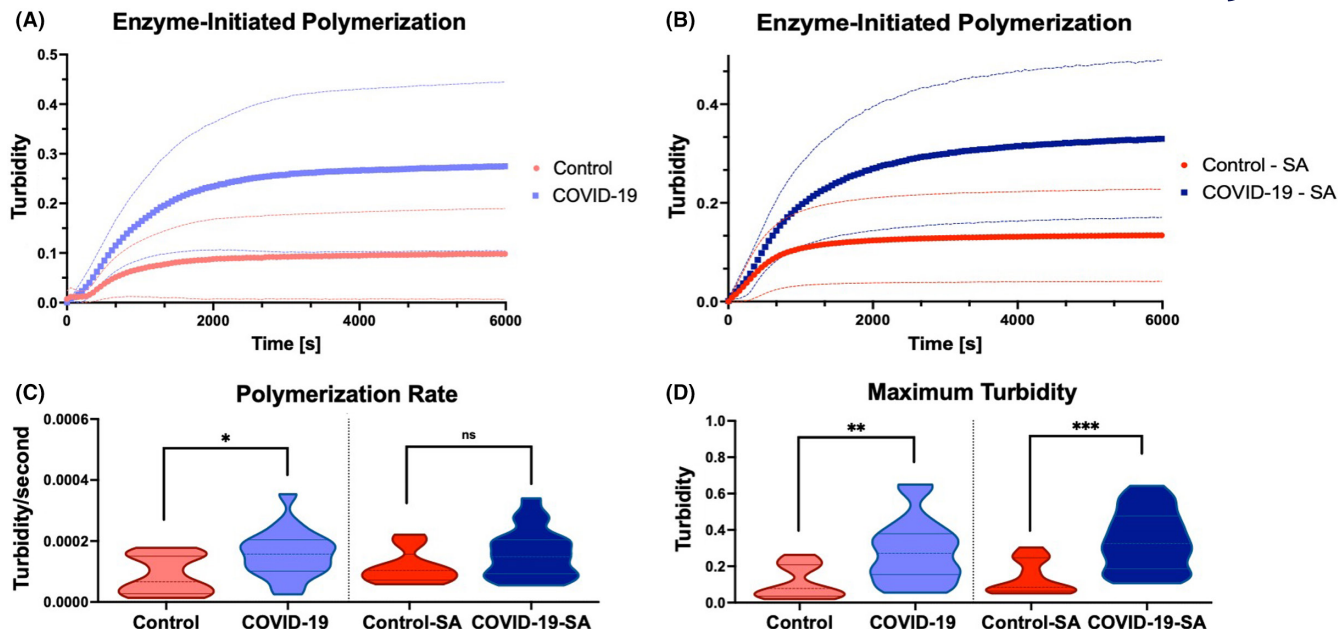
FIGURE 4 Enzyme-initiated polymerization of COVID-19 and control fibrin clots, at baseline and with sialic acid residues removed. (A) Enzyme-initiated polymerization curves for COVID-19 and control fibrinogen. Thrombin (0.5 U/ml) was added to 2 mg/ml fibrinogen to provoke clot formation, and a plate reader was used to produce turbidity curves demonstrating fibrin clot polymerization. $N = 6–9$. (B) Enzyme-initiated polymerization curves for desialylated COVID-19 and control fibrinogen. Thrombin (0.5 U/ml) was added to 2 mg/ml fibrinogen to induce clot formation, and a plate reader was used to produce turbidity curves demonstrating fibrin clot polymerization. $N = 6–9$. (C) Comparison of maximum turbidity achieved for COVID-19 and control, and desialylated COVID-19 and control enzyme-initiated polymerization turbidity curves. $N = 6–9$. (D) Comparison of polymerization rate for COVID-19 and control, and desialylated COVID-19 and control enzyme-initiated polymerization turbidity curves. Polymerization rate was determined as the slope of the curve at half of the maximum turbidity. $N = 6–9$ $N = 6–9$. $*p < .05$, $**p < .01$, $***p < .005$.

The altered fibrinogen structure in COVID-19 patients has important clinical implications for the treatment of thrombotic complications. The differing clot properties are likely to make these clots less permeable because of their decreased porosity, and therefore more resistant to treatment via thrombolytic therapy. The density of a clot can also have implications for the formation of fibrosis and adherence to vessel walls,[33] which may have clinical implications for surgical removal procedures. The difference in results between endogenous and exogenous fibrinolysis assays suggests that while differences in density and porosity are likely contributors to differences in fibrinolytic rates, there are undeniably other unexplored factors at play as well. However, in both endogenous and exogenous assays, COVID-19 samples degraded significantly faster after desialylation, indicating that SA residues play some role in these multifactorial influences. The degradation assays we performed investigated instantaneous degradation rate; however, these data also support fibrinogen structure as partial explanation for previous findings that overall clot persistence and total time to degrade is higher among COVID-19 plasma.[34] Our findings that area under the curve is significantly greater for COVID-19 patients alongside the visualizations of clot degradation (Figures 3A and 5A) are consistent with findings that COVID-19 clots persist for longer than control clots during *ex vivo* degradation studies.[34] This work evaluates isolated fibrinogen without the influence of other plasma factors. As such, some measure of difference in findings from studies of *in vivo*

clotting in COVID-19 patients or of patient whole blood or plasma is expected and can be attributed to the additional elements at play in those samples.

We also measured differences in the sialic acid content of fibrinogen from COVID-19 samples and assessed the role of SA residues in clot dynamics. We show for the first time that fibrinogen isolated from COVID-19 patients has significantly more SA content than fibrinogen collected from noninfected adults. Furthermore, the presence of SA is at the center of the changes in clot density observed in COVID-19 fibrin clots because removal of SA resolved intergroup differences in clot density. Desialylation also lead to an increase in instantaneous degradation rate when compared with the unaltered COVID-19 fibrinogen. This makes sense because decreased density is associated with increased porosity, which should lead to improved clot permeability to external lytic agents. However, when SA was removed from COVID-19 fibrinogen, no meaningful changes in clot polymerization dynamics occurred. The desialylated COVID-19 fibrinogen continued to polymerize faster and reach a higher clot turbidity than the desialylated control fibrinogen. This suggests that additional structural changes in COVID-19 fibrinogen remain to be identified. Our results show clear differences between COVID-19 and control fibrinogen, which is a strong indicator that posttranslational modification, and possibly viral modification, affect fibrinogen during active SARS-CoV-2 infection. However, more work is certainly needed to parse the, likely multifactorial, causes of these
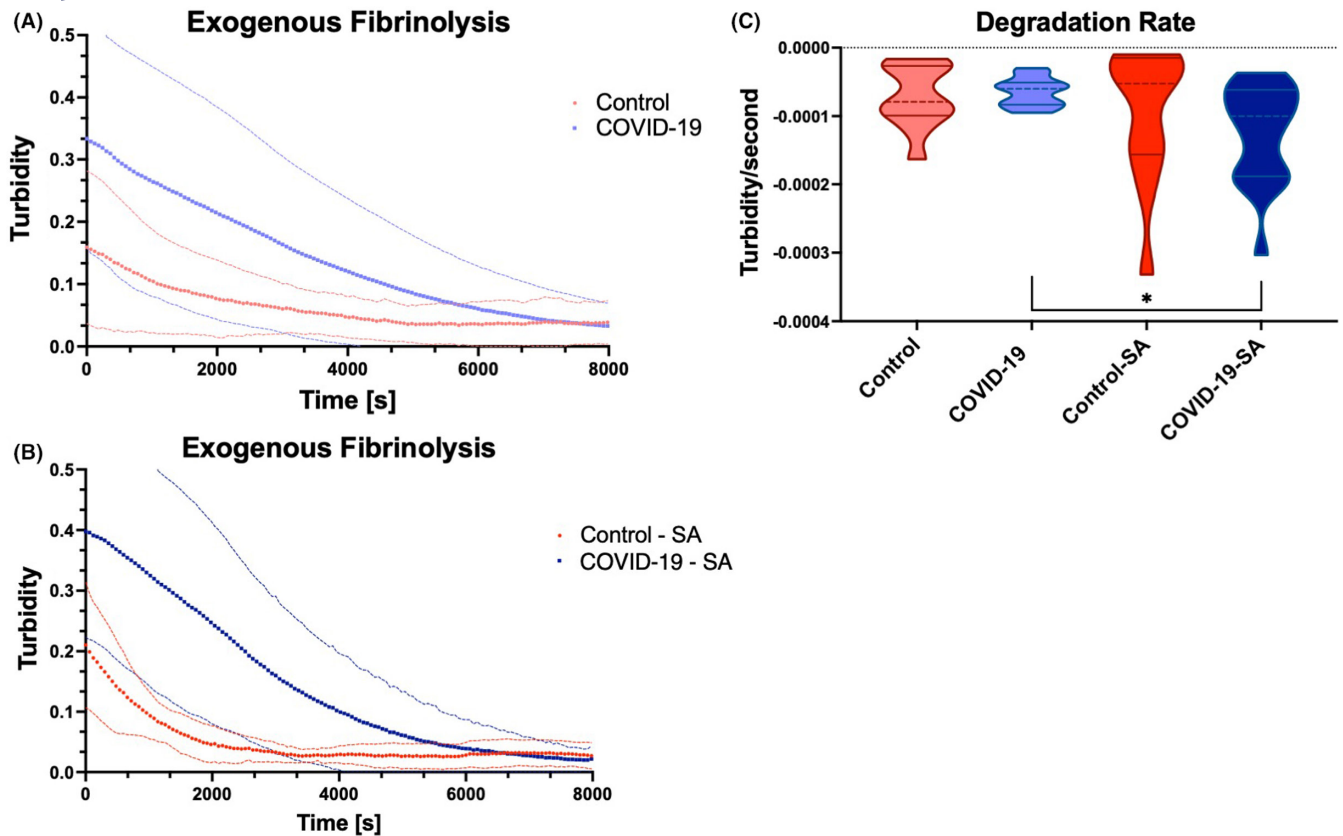
FIGURE 5 Exogenous fibrinolysis of COVID-19 and control fibrin clots, at baseline and with sialic acid residues removed. (A) Exogenous fibrinolysis curves for COVID-19 and control fibrinogen. A plasmin overlay (0.5 U/ml) was added to fully polymerized fibrinogen (2 mg/ml) clots to induce fibrinolysis, and a plate reader was used to produce turbidity curves demonstrating fibrin clot degradation. $N = 6–9$. (B) Exogenous fibrinolysis curves for desialylated COVID-19 and control fibrinogen. The same process was used as described in (A). $N = 6–9$. (C) Comparison of instantaneous degradation rate for COVID-19 and control exogenous fibrinolysis turbidity curves, both at baseline and after the removal of sialic acid residues. $N = 6–9$. *$p < .05$, **$p < .01$, ***$p < .005$.

structural differences in fibrinogen. Direct viral induction of fibrinogen molecular changes should also be explored as a potential cause of differences seen in COVID-19 clots. This may be done through direct exposure of healthy plasma to COVID-19 viral particles and subsequent analysis of the resultant fibrinogen.

This study is limited by the use of only COVID-19 plasma samples from patients with severe symptoms that require ICU-level care. Future studies should look at comparing ICU, hospitalized, and outpatient COVID-19 samples as a proxy for illness severity. Another limitation lies in the use of a single control group composed of a mixture of ICU patients and healthy controls. Future studies would benefit from the use of control groups to compare with both noninfected ICU patients and healthy controls separately to further validate that the novel structure described herein is not merely a reflection of disease severity. Additionally, as previously noted, coagulative irregularities have been implicated in the symptomatology of long COVID.[14–16] Although all of the experimental samples collected for this study were from patients with active COVID-19 infection, future studies should investigate the persistence of this COVID-19-type fibrinogen in the plasma of recovered COVID-19 patients at different time points, as well as patients identified as likely suffering from long COVID symptoms.

Differential sialylation has been previously determined to produce the structural and kinetic differences observed between adult and neonatal fibrinogen.[23] Previous findings have also noted that when mixed, neonatal and adult fibrinogen do not fully integrate together, instead forming fibrinogen subpopulations during clot formation.[35] This has significant clinical implications for neonatal hemostasis following the administration of blood products because these products necessarily come from adult donors. As differential SA content is likely to be the cause of this, it is an important consideration that healthy adult blood products may not seamlessly integrate into the blood of COVID-19 patients, and more research is needed to determine whether complications with differential sialylation between a blood donor and blood recipient might affect the recipient's thrombotic risk. Additionally, some data indicate that children younger than age 12 years infected with SARS-CoV-2 are less likely to suffer from thrombotic complications than those older than 12 years old.[36] It is possible that differential sialylation from immature fibrinogen may play at least some role in this difference in risk. Future studies should investigate fibrinogen changes in children of different ages with COVID-19.

Our studies have demonstrated differences between COVID-19 and control fibrinogen, but our findings of differential SA content have only partially explained the differences that we note herein. Although

structural differences in COVID-19 fibrin clots, and to a certain extent changes in degradation, can be explained by the differential SA content of this fibrinogen, these changes were not responsible for the significant difference in fibrin polymerization noted in these studies. As such, the observed changes are almost certainly multifactorial in nature, and other known posttranslational modifications of fibrinogen, including oxidation, nitration, phosphorylation, and acetylation should be investigated.[19,37] Tandem mass spectroscopy might be particularly useful for this because it can provide information on both the type and location of posttranslational molecular modifications. Also of note, although we have demonstrated a significant difference in sialic acid residues in COVID-19 fibrinogen, we have not identified their location within the molecular structure, nor have we determined the mechanism of their effect on clot structure in this case. Affinity, electrostatic charge, and steric hindrance are all plausible mechanisms for the changes noted, and additional work will be needed to fully understand the underlying processes. Future studies are also indicated to explore these questions and potential differences in the structure and function of factors II, VII, IX, XIII, and plasminogen, are also warranted, as these all interact with fibrinogen during clot polymerization.

In summary, our data indicate that clots made from the fibrinogen of patients being treated for COVID-19 display significantly altered pro-thrombotic qualities: increased density and stiffness, increased rate of polymerization, and greater ultimate clot turbidity. This provides clear evidence that altered fibrinogen structure in COVID-19 patients is a contributing factor to thrombogenic characteristics of the disease. We have also shown that COVID-19 fibrinogen has greater amount of sialic acid residues, and that the removal of these residues results in the resolution of differences in clot density. The removal of these sialic acid residues also resulted in increased rate of clot degradation compared with the unaltered COVID-19 fibrinogen; however, differences in polymerization and clot turbidity remained. As such, differential sialylation of COVID-19 fibrinogen likely mediates differences in structure, and to some extent differences in degradation, but additional structural differences must be investigated.

AUTHOR CONTRIBUTIONS

N.M. performed experiments, analyzed results, and wrote the paper; N.Z. assisted in clot structure and degradation experiments; R.S. and F.S. assisted in research design and paper writing; and A.C.B. designed and supervised the study, performed data analysis, and wrote the paper.

ACKNOWLEDGMENTS

CONFLICT OF INTEREST

A.C.B. is founder and chief executive officer of Selsym Biotech, Inc., a startup company focused developing fibrin-targeted hemostatic agents. All other authors declare no competing financial interests.

ORCID

Nina Moiseiwitsch https://orcid.org/0000-0001-7406-0258
Nicole Zwennes https://orcid.org/0000-0001-6928-9349
Fania Szlam https://orcid.org/0000-0002-2314-9428
Roman Sniecinski https://orcid.org/0000-0003-4766-3314
Ashley Brown https://orcid.org/0000-0001-6995-1785

REFERENCES

1. Clarke KEN, Jones JM, Deng Y, et al. Seroprevalence of infection-induced SARS-CoV-2 antibodies - United States, September 2021–February 2022. *MMWR Morb Mortal Wkly Rep.* 2022;71:606-608. doi:10.15585/mmwr.mm7117e3
2. Burn E, Duarte-Salles T, Fernandez-Bertolin S, et al. Venous or arterial thrombosis and deaths among COVID-19 cases: a European network cohort study. *Lancet Infect Dis.* 2022;22:1142-1152. doi:10.1016/s1473-3099(22)00223-7
3. Bikdeli B, Madhavan MV, Jimenez D, et al. COVID-19 and thrombotic or thromboembolic disease: implications for prevention, antithrombotic therapy, and follow-up: JACC state-of-the-art review. *J Am Coll Cardiol.* 2020;75:2950-2973. doi:10.1016/j.jacc.2020.04.031
4. Tan BK, Mainbourg S, Friggeri A, et al. Arterial and venous thromboembolism in COVID-19: a study-level meta-analysis. *Thorax.* 2021;76:970-979. doi:10.1136/thoraxjnl-2020-215383
5. Reilev M, Kristensen KB, Pottegård A, et al. Characteristics and predictors of hospitalization and death in the first 11 122 cases with a positive RT-PCR test for SARS-CoV-2 in Denmark: a nationwide cohort. *Int J Epidemiol.* 2020;49:1468-1481. doi:10.1093/ije/dyaa140
6. Zhou F, Yu T, Du R, et al. Clinical course and risk factors for mortality of adult inpatients with COVID-19 in Wuhan, China: a retrospective cohort study. *Lancet.* 2020;395:1054-1062. doi:10.1016/s0140-6736(20)30566-3
7. Gupta S, Hayek SS, Wang W, et al. Factors associated with death in critically ill patients with coronavirus disease 2019 in the US. *JAMA Intern Med.* 2020;180:1436-1447. doi:10.1001/jamainternmed.2020.3596
8. Katsoularis I, Fonseca-Rodríguez O, Farrington P, et al. Risks of deep vein thrombosis, pulmonary embolism, and bleeding after covid-19: nationwide self-controlled cases series and matched cohort study. *BMJ.* 2022;377:e069590. doi:10.1136/bmj-2021-069590
9. Barrett TJ, Cornwell M, Myndzar K, et al. Platelets amplify endotheliopathy in COVID-19. *Sci Adv.* 2021;7:eabh2434. doi:10.1126/sciadv.abh2434
10. Bonaventura A, Vecchié A, Dagna L, et al. Endothelial dysfunction and immunothrombosis as key pathogenic mechanisms in COVID-19. *Nat Rev Immunol.* 2021;21:319-329. doi:10.1038/s41577-021-00536-9
11. Canzano P, Brambilla M, Porro B, et al. Platelet and endothelial activation as potential mechanisms behind the thrombotic complications of COVID-19 patients. *JACC Basic Transl Sci.* 2021;6:202-218. doi:10.1016/j.jacbts.2020.12.009
12. Lazzaroni MG, Piantoni S, Masneri S, et al. Coagulation dysfunction in COVID-19: the interplay between inflammation, viral infection and the coagulation system. *Blood Rev.* 2021;46:100745. doi:10.1016/j.blre.2020.100745
13. Iba T, Levy JH, Levi M, Thachil J. Coagulopathy in COVID-19. *J Thromb Haemost.* 2020;18:2103-2109. doi:10.1111/jth.14975
14. Kell DB, Laubscher GJ, Pretorius E. A central role for amyloid fibrin microclots in long COVID/PASC: origins and therapeutic implications. *Biochem J.* 2022;479:537-559. doi:10.1042/bcj20220016
15. Renzi S, Landoni G, Zangrillo A, Ciceri F. MicroCLOTS pathophysiology in COVID 19. *Korean J Intern Med.* 2020. doi:10.3904/kjim.2020.336

16. de Vries JJ, Visser C, Geers L, et al. Altered fibrin network structure and fibrinolysis in intensive care unit patients with COVID-19, not entirely explaining the increased risk of thrombosis. *J Thromb Haemostasis*. 2022;20:1412-1420. doi:10.1111/jth.15708

17. Maier CL, Sarker T, Szlam F, Sniecinski RM. COVID-19 patient plasma demonstrates resistance to tPA-induced fibrinolysis as measured by thromboelastography. *J Thromb Thrombolysis*. 2021;52:766-771. doi:10.1007/s11239-021-02438-y

18. Stefely JA, Christensen BB, Gogakos T, et al. Marked factor V activity elevation in severe COVID-19 is associated with venous thromboembolism. *Am J Hematol*. 2020;95:1522-1530. doi:10.1002/ajh.25979

19. Vries JJD, Snoek CJM, Rijken DC, Maat MPMD. Effects of post-translational modifications of fibrinogen on clot formation, clot structure, and fibrinolysis. *Arterioscler Thromb Vasc Biol*. 2020;40:554-569. doi:10.1161/ATVBAHA.119.313626

20. Okude M, Yamanaka A, Morimoto Y, Akihama S. Sialic acid in fibrinogen: effects of sialic acid on fibrinogen-fibrin conversion by thrombin and properties of asialofibrin clot. *Biol Pharm Bull*. 1993;16:448-452. doi:10.1248/bpb.16.448

21. Dang CV, Shin CK, Bell WR, Nagaswami C, Weisel JW. Fibrinogen sialic acid residues are low affinity calcium-binding sites that influence fibrin assembly. *J Biol Chem*. 1989;264:15104-15108.

22. Martinez J, MacDonald KA, Palascak JE. The role of sialic acid in the dysfibrinogenemia associated with liver disease: distribution of sialic acid on the constituent chains. Blood 1983;61:1196–202.

23. Nellenbach K, Kyu A, Guzzetta N, Brown AC. Differential sialic acid content in adult and neonatal fibrinogen mediates differences in clot polymerization dynamics. *Blood Adv*. 2021;5:5202-5214. doi:10.1182/bloodadvances.2021004417

24. Qiu LL, Levinson SS, Keeling KL, Elin RJ. Convenient and effective method for removing fibrinogen from serum specimens before protein electrophoresis. *Clin Chem*. 2003;49:868-872. doi:10.1373/49.6.868

25. Dietrich M, Heselhaus J, Wozniak J, et al. Fibrin-based tissue engineering: comparison of different methods of autologous fibrinogen isolation. *Tissue Eng Part C Methods*. 2013;19:216-226. doi:10.1089/ten.TEC.2011.0473

26. Aper T, Kolster M, Hilfiker A, Teebken O, Haverich A. Fibrinogen preparations for tissue engineering approaches. *J Bioeng Biomed Sci*. 2012;2:115.

27. Diaz-Mauriño T, Castro C, Albert A. Desialylation of fibrinogen with neuraminidase. Kinetic and clotting studies. *Thromb Res*. 1982;27:397-403. doi:10.1016/0049-3848(82)90057-3

28. Nellenbach K, Guzzetta NA, Brown AC. Analysis of the structural and mechanical effects of procoagulant agents on neonatal fibrin networks following cardiopulmonary bypass. *J Thromb Haemost*. 2018;16:2159-2167. doi:10.1111/jth.14280

29. Sproul EP, Hannan RT, Brown AC. Controlling fibrin network morphology, polymerization, and degradation dynamics in fibrin gels for promoting tissue repair. *Methods Mol Biol*. 2018;1758:85-99. doi:10.1007/978-1-4939-7741-3_7

30. Valladolid C, Martinez-Vargas M, Sekhar N, et al. Modulating the rate of fibrin formation and clot structure attenuates microvascular thrombosis in systemic inflammation. *Blood Adv*. 2020;4:1340-1349. doi:10.1182/bloodadvances.2020001500

31. Sproul EP, Nandi S, Chee E, et al. Development of biomimetic antimicrobial platelet-like particles comprised of microgel nanogold composites. *Regen Eng Transl Med*. 2020;6:299-309. doi:10.1007/s40883-019-00121-6

32. Sproul EP, Nandi S, Roosa C, Schreck L, Brown AC. Biomimetic microgels with controllable deformability improve healing outcomes. *Adv Biosyst*. 2018;2:1800042. doi:10.1002/adbi.201800042

33. Dawson DL, Ronningen E. Vascular laboratory: venous duplex scanning. In: Sidawy AN, Perler BA, eds. *Rutherford's Vascular Surgery and Endovascular Therapy*. 9th ed. Elsevier; 2019:246-264.e4.

34. Fan BE, Ng J, Chan SSW, et al. COVID-19 associated coagulopathy in critically ill patients: a hypercoagulable state demonstrated by parameters of haemostasis and clot waveform analysis. *J Thromb Thrombolysis*. 2021;51:663-674. doi:10.1007/s11239-020-02318-x

35. Brown AC, Hannan RT, Timmins LH, Fernandez JD, Barker TH, Guzzetta NA. Fibrin network changes in neonates after cardiopulmonary bypass. *Anesthesiology*. 2016;124:1021-1031. doi:10.1097/aln.0000000000001058

36. Whitworth H, Sartain SE, Kumar R, et al. Rate of thrombosis in children and adolescents hospitalized with COVID-19 or MIS-C. *Blood*. 2021;138:190-198. doi:10.1182/blood.2020010218

37. Hugenholtz GC, Macrae F, Adelmeijer J, et al. Procoagulant changes in fibrin clot structure in patients with cirrhosis are associated with oxidative modifications of fibrinogen. *J Thromb Haemost*. 2016;14:1054-1066. doi:10.1111/jth.13278

SUPPORTING INFORMATION

Additional supporting information can be found online in the Supporting Information section at the end of this article.

How to cite this article: Moiseiwitsch N, Zwennes N, Szlam F, Sniecinski R, Brown A. COVID-19 patient fibrinogen produces dense clots with altered polymerization kinetics, partially explained by increased sialic acid. *J Thromb Haemost*. 2022;00:1-12. doi: 10.1111/jth.15882